Nonreciprocal Superradiant Phase Transitions and Multicriticality in a Cavity QED System

Gui-Lei Zhu,[1,2] Chang-Sheng Hu,[3] Hui Wang,[2] Wei Qin,[2,4] Xin-You Lü,[5,*] and Franco Nori[2,6,7,†]

[1]*Department of Physics, Zhejiang Sci-Tech University, Hangzhou 310018, China*
[2]*Theoretical Quantum Physics Laboratory, Cluster for Pioneering Research, RIKEN, Wakoshi, Saitama 351-0198, Japan*
[3]*Department of Physics, Anhui Normal University, Wuhu 241000, China*
[4]*Center for Joint Quantum Studies and Department of Physics, School of Science, Tianjin University, Tianjin 300350, China*
[5]*School of Physics, Huazhong University of Science and Technology and Wuhan Institute of Quantum Technology, Wuhan 430074, China*
[6]*Quantum Computing Center, RIKEN, Wakoshi, Saitama 351-0198, Japan*
[7]*Department of Physics, The University of Michigan, Ann Arbor, Michigan 48109-1040, USA*

(Received 18 July 2023; revised 6 February 2024; accepted 1 April 2024; published 7 May 2024)

We demonstrate the emergence of nonreciprocal superradiant phase transitions and novel multicriticality in a cavity quantum electrodynamics system, where a two-level atom interacts with two counterpropagating modes of a whispering-gallery-mode microcavity. The cavity rotates at a certain angular velocity and is directionally squeezed by a unidirectional parametric pumping $\chi^{(2)}$ nonlinearity. The combination of cavity rotation and directional squeezing leads to nonreciprocal first- and second-order superradiant phase transitions. These transitions do not require ultrastrong atom-field couplings and can be easily controlled by the external pump field. Through a full quantum description of the system Hamiltonian, we identify two types of multicritical points in the phase diagram, both of which exhibit controllable nonreciprocity. These results open a new door for all-optical manipulation of superradiant transitions and multicritical behaviors in light-matter systems, with potential applications in engineering various integrated nonreciprocal quantum devices.

DOI: 10.1103/PhysRevLett.132.193602

Phase transitions and critical phenomena are at the heart of understanding the nature of the matter in condensed matter physics and material science [1,2]. One of the most intriguing topics in light-matter systems is the superradiant phase transition [3–5], where increasing the atom-field coupling through a critical value induces a transition from the normal phase (NP) to the superradiant phase (SP) [6–15]. This superradiant transition typically occurs in the thermodynamic limit, where the number of atoms N approaches infinity. In the quantum Rabi model [16–18] with $N = 1$, a similar transition can occur, but it requires both ultrastrong light-matter coupling and an extremely large atomic frequency [19–26]. The realization of the phase transition in such single-atom models has been successfully demonstrated in quantum simulation platforms, including nuclear magnetic resonance (NMR) quantum simulators [27,28], driven atoms in trapped ions [29,30], and superconducting qubits [31].

In open systems, the presence of photon loss can have a significant impact on the critical behavior of the Hamiltonian part of the system [32,33]. It can induce multicritical phenomena [34–38] or even completely suppress its criticality [39]. In addition, this class of driven-dissipative systems allows for the demonstration of richer physics, such as the breakdown of photon blockade [40–42], stable superradiant lasers [43–46], time crystals [47–49], and atomic synchronization [50,51]. However, thus far, the realization of superradiant transitions has not simultaneously combined the features necessary for exquisite controllability, such as strong nonreciprocity, tunability, and compact integration.

Optical nonreciprocity [52–63] is characterized by the asymmetric behavior of optical signals as they travel through an optical system in opposite directions. This phenomenon plays a crucial role in optical information processing and quantum networks [64–66]. Notably, a theory of nonreciprocal phase transitions in nonequilibrium systems has been proposed, suggesting that asymmetric couplings of multiple species can give rise to time-dependent phases [67]. Recently, this concept has been applied to the Dicke model with two spin species [68]. Yet, the technique used to achieve nonreciprocal phase transition in these schemes is not readily applicable to achieving *controllable* nonreciprocal transitions in a light-matter system. In general, achieving the superradiant transition requires tunability of the dipole coupling of the radiation field to atoms. To this end, many pioneering approaches have been proposed, including stimulated Raman transitions [69–71] and quantum simulators [28,31,72]. However, breaking the reciprocity of the system, in these approaches, remains challenging. The exquisite control of superradiant transitions and multicriticality through external fields is an intriguing topic and may inspire new applications, such as on-chip unidirectional superradiant lasers [43–46] and integrated high-precision quantum sensing [73–76].

In this Letter, inspired by recent experimental advances [77–84] and related works [85,86], we propose an experimentally feasible approach for all-optical control of superradiant phase transitions in a cavity quantum electrodynamics (QED) system. Our method focuses on a rotating dual-coupling Jaynes-Cummings (JC) model, where the clockwise and counterclockwise resonator modes are simultaneously coupled to a two-level atom. Generally, the JC model does not exhibit superradiant transitions in the presence of cavity dissipation [39]. Here, we revive such transitions by introducing a classical field to subtly parametrically pump one of the cavity modes. This driven-dissipative setup enables steady-state superradiant transitions to occur in the experimentally friendly cavity QED system, which do not require ultrastrong coupling strengths, and the extremely large atomic detuning can be easily achieved by tuning the external pump field. This all-optical control has some main advantages compared to its magnetic and electronic counterparts, such as compactness, ease of integration, and lower power consumption (see Sec. S7. B in Supplemental Material [87]).

Interestingly, the combination of cavity rotation [84,110–112] and directional squeezing causes the critical points of phase transitions to shift in opposite directions. As a result, the system exhibits nonreciprocal first- and second-order superradiant phase transitions. Moreover, we observe a rich phase diagram featuring a controllable tricritical point and multicritical points, all displaying nonreciprocity. Our Letter fundamentally combines the theories of phase transitions and multicriticality with nonreciprocal physics and could provide valuable resources for quantum metrology [113].

Model.—Here, we consider the model of a two-level atom interacting with two counterpropagating modes of a whispering-gallery-mode (WGM) resonator, as depicted in Figs. 1(a) and 1(b). The resonator is made of materials with second-order ($\chi^{(2)}$) nonlinearity [114,115]. A classical field at frequency ω_p is input from either forward or backward to drive the nonlinearity, which generates directional squeezing cavity modes through an optical parametric amplification (OPA) process [63,116–121] (see Sec. S9. B in [87]). The resonator rotates counterclockwise with an angular velocity, denoted as Ω. This rotation can be experimentally achieved by mounting the resonator on a turbine [84] (see Sec. S9. C in [87]). Therefore, the two cavity modes undergo Sagnac-Fizeau shifts concerning their static resonance frequency, represented by ω_0 [84,122], i.e., $\omega_0 \to \omega_0 \pm \Delta_F$, with $\Delta_F \approx nR\Omega\omega_0(1-n^{-2})/c$. Here n and R present the refractive index and radius of the resonator, and c is the speed of light. Note that a positive Sagnac-Fizeau shift ($\Delta_F > 0$) corresponds to the forward pump case, while a negative shift ($\Delta_F < 0$) corresponds to the backward pump.

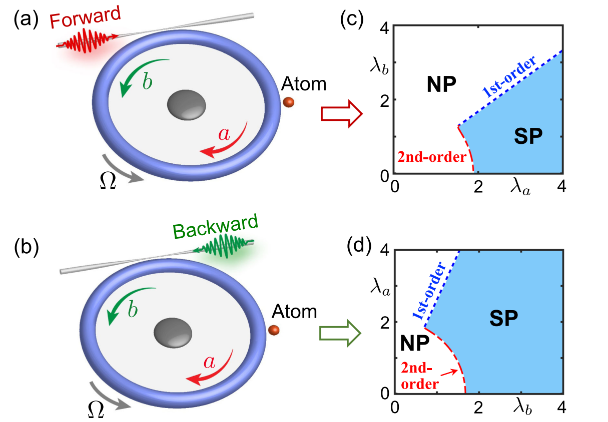

FIG. 1. Schematic illustration of the rotating dual-coupling JC model in the forward (a) and backward (b) pumps. The WGM resonator with $\chi^{(2)}$ nonlinearity embedded (not shown here), supports counterclockwise and clockwise cavity modes labeled as a and b respectively, and both modes interact with a two-level atom. The resonator rotates counterclockwise at an angular velocity Ω. (c),(d) Boundaries of the NP and SP for forward and backward pumps, respectively. The parameters used here are $\Delta = 2$, $\kappa/\Delta = 0.05$, $G/\kappa = 1.5$, $J = 0$, and $\Delta_F/\Delta = 0.5$ in (c) and $\Delta_F/\Delta = -0.5$ in (d).

In the frame rotating at $\omega_p/2$, the dual-coupling JC Hamiltonian with the forward pump is given by ($\hbar = 1$)

$$\begin{aligned} H &= H_0 + H_{\text{int}}, \\ H_0 &= (\Delta+\Delta_F)a^\dagger a + (\Delta-\Delta_F)b^\dagger b + \frac{\Delta_q}{2}\sigma_z + G(a^{\dagger 2}+a^2), \\ H_{\text{int}} &= [(g_a a + g_b b)\sigma_+ + J a^\dagger b + \text{H.c.}], \end{aligned} \tag{1}$$

where a and b are the annihilation operators of the counterclockwise and clockwise cavity modes, respectively, and $\sigma_\pm = (\sigma_x \pm i\sigma_y)/2$ are the atomic Pauli matrices. The detunings are defined as $\Delta = \omega_0 - \omega_p/2$ and $\Delta_q = \omega_q - \omega_p/2$. The cavity modes a and b are coupled to the atom with strengths g_a and g_b, respectively, and $G(a^{\dagger 2} + a^2)$ is the two-photon drive term generated from the OPA process, with G representing the pump strength. In our analytical calculations, the focus is on the forward pump case, and the backward Hamiltonian can be obtained by replacing the two-photon term with $G(b^{\dagger 2} + b^2)$. The parameter J represents the hopping amplitude between two cavity modes, and for simplicity, we assume $J = 0$ in the following analytical derivations, as it does not affect the main results (see Sec. S8 in [87]).

Taking into account both the cavity and atomic dissipation, the system evolution is described by the master equation,

$$\frac{d\rho}{dt} = -i[H,\rho] + \kappa\mathcal{D}[a] + \kappa\mathcal{D}[b] + \gamma\mathcal{D}[\sigma_-], \qquad (2)$$

where ρ is the density matrix of the system, and $\mathcal{D}[o] = 2o\rho o^\dagger - (o^\dagger o\rho + \rho o^\dagger o)$ is the Lindblad superoperator. Here, we have assumed equal decay rates for the two cavity modes ($\kappa_a = \kappa_b = \kappa$). To ensure the conservation of the total pseudoangular momentum, we focus mainly on the effect of cavity dissipation and set the atomic decay rate $\gamma = 0$.

The presence of dissipation, as discussed in [39], can completely suppress the superradiant transition in the JC model. Interestingly, in our model, the two-photon drive is capable of resurrecting this transition. From a symmetry perspective, the two-photon term changes the system from a continuous U(1) symmetry to a discontinuous Z_2 symmetry. This Z_2 symmetry is defined by $[H,\Pi] = 0$ with the parity operator $\Pi = \exp\{i\pi N\}$, where $N = a^\dagger a + b^\dagger b + (\sigma_z + 1)/2$ is the total number of excitations in the system [19]. We define the ratios between the atomic detuning and cavity detuning as $\eta_\pm = \Delta_q/(\Delta \pm \Delta_F)$, and $\mu = \Delta_q/G$. Note that the limit of $\eta_\pm \to \infty$ is physically similar to the infinite-frequency limit in the standard Rabi model ($\omega_q/\omega_0 \to \infty$). Fortunately, in our model, this limit can be easily achieved by tuning the pump frequency ω_q. For convenience, we introduce the dimensionless atom-field couplings as $\lambda_{a,b} = 2g_{a,b}/\sqrt{\Delta_q(\Delta \pm \Delta_F)}$. These couplings are determined by the detunings Δ_q and Δ, rather than the atomic frequency ω_q and resonator frequency ω_0. Thus, our approach relaxes the couplings required for the superradiant phase transitions from the ultrastrong coupling regime to the strong coupling regime (see Sec. S7. A in [87]). In the large atomic detuning limit, $\eta_\pm \to \infty$ and $\mu \to \infty$, when the couplings λ_a, λ_b increase beyond their critical values, the system undergoes a Rabi-like phase transition from the NP to the SP, indicating the breaking of Z_2 symmetry.

Nonreciprocal superradiant phase transitions.— According to Eq. (2), we obtain a set of Heisenberg equations of motion for operators (see Sec. S1 in [87]). We define the renormalized occupation of the cavity modes as $\langle a\rangle = \alpha\sqrt{\eta_+}$ and $\langle b\rangle = \beta\sqrt{\eta_-}$, with $\alpha = \alpha_{\rm Re} + i\alpha_{\rm Im}$, $\beta = \beta_{\rm Re} + i\beta_{\rm Im}$. In the long-time limit, the system reaches a steady state and we can obtain the mean-field solutions for cavity occupations $\alpha_{\rm Re}, \alpha_{\rm Im}$ and $\beta_{\rm Re}, \beta_{\rm Im}$ [87]. The validity of the mean-field approach is discussed in Sec. S6 in [87]. When $\alpha_{\rm Re}, \alpha_{\rm Im}, \beta_{\rm Re}, \beta_{\rm Im} = 0$, the system is in the NP, while nonzero values of $\alpha_{\rm Re}$, $\alpha_{\rm Im}$, $\beta_{\rm Re}$, $\beta_{\rm Im}$ indicate the SP. Figures 1(c) and 1(d) display the phase diagrams of $\alpha_{\rm Re}, \alpha_{\rm Im}$ and $\beta_{\rm Re}, \beta_{\rm Im}$, for the forward and backward pumps, respectively. When the pump strength is fixed at $G/\kappa = 1.5$, the first- (and second-) order transition boundary differs between the two pump directions, leading to the nonreciprocity of the superradiant transitions (see below). Here, the first- and second-order transition boundaries are, respectively, characterized by

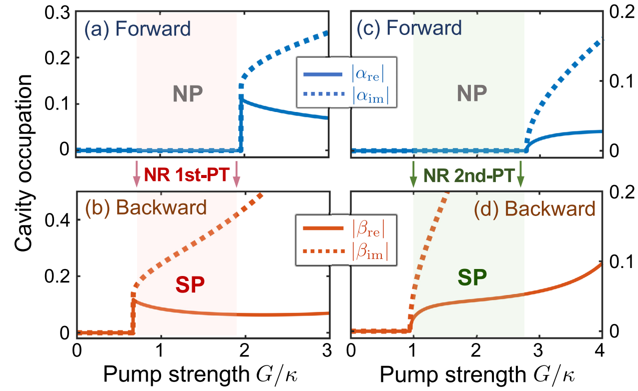

FIG. 2. The cavity occupations α and β versus the pump strength G/κ, for both the forward and backward pumps. The solid (or dotted) curve denotes the real (or imaginary) part of cavity occupations. In (a),(b), where $\lambda = 1.5$, the shaded areas indicate the nonreciprocal first-order phase transition (NR 1st PT). In (c),(d), where $\lambda = 1.36$, the shaded areas indicate the nonreciprocal second-order phase transition (NR 2nd PT). Here, $\Delta_F/\Delta = \pm 0.5$ for the forward and backward pumps, respectively, $\lambda_a = \lambda_b = \lambda$, and other parameters are the same as in Fig. 1.

discontinuous jumps and continuous changes in the cavity occupations (see Fig. S1 in [87]).

To enable all-optical manipulation of superradiant phase transitions using an external field, we simplify the system by adjusting $\lambda_a = \lambda_b = \lambda$. In this configuration, with a fixed coupling λ, increasing the pump strength G beyond a critical value can induce either a first- or second-order phase transition. The respective critical pump strengths can be analytically calculated as (see Sec. S3 in [87])

$$G_c^{\rm first} = \frac{1}{4\kappa\Delta_-}\left[-u + \sqrt{(u + 2\Delta_-\kappa^2)^2 + 4\Delta_+^2\Delta_-^2\kappa^2}\right], \qquad (3)$$

$$G_c^{\rm second} = \frac{[\Delta^4 p^2 + (2\kappa^2 - \Delta_F^2 p)^2 + \Delta^2(qp^2 + 4\kappa^2)]^{1/2}}{[16\kappa^2 + \Delta_-^2(p-2)^2]^{1/2}}, \qquad (4)$$

where $\Delta_\pm = \Delta \pm \Delta_F$, $u = \Delta_+(\Delta_-^2 + \kappa^2)$, $q = \kappa^2 - 2\Delta_F^2$, and $p = \lambda^2 - 2$. Notably, the first-order critical pump strength $G_c^{\rm first}$ is irrelevant to the coupling λ. By setting $G_c^{\rm first} = G_c^{\rm second}$, the tricritical point can be determined at $\lambda_{\rm tric} \approx \sqrt{2}$ [see Fig. S2(b) in [87] for details].

Figure 2 shows the cavity occupations α and β versus the pump strength G. In the left panel, we consider the case of $\lambda = 1.5$. When the system is driven by a forward pump [Fig. 2(a)], the cavity occupations exhibit a discontinuous jump from zero to finite values, when G exceeds a critical value $G_{\rm c,f}^{\rm first} = 1.96\kappa$ (located near the right edge of the shaded region). This is evidence of a first-order phase transition. However, when driven by a backward pump [Fig. 2(b)], the critical value is shifted to $G_{\rm c,b}^{\rm first} = 0.66\kappa$, the

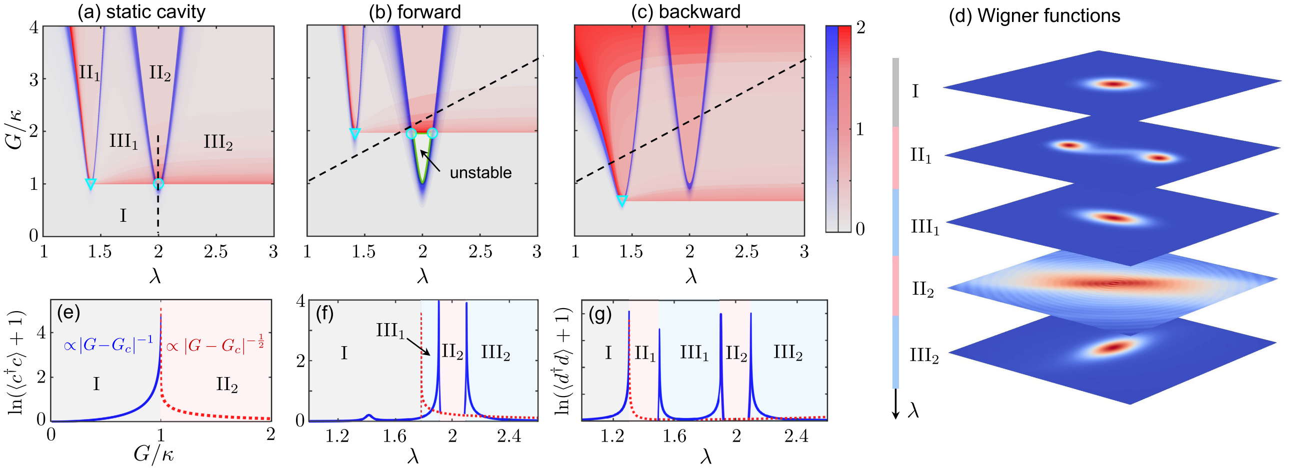

FIG. 3. (a)–(c) Phase diagram of the steady-state photon number fluctuations, with $\langle c^\dagger c\rangle$ for the forward (b), $\langle d^\dagger d\rangle$ for the backward (c), and $\langle c^\dagger c\rangle$ (or $\langle d^\dagger d\rangle$) for the static microcavity (a). The blue (red) bar represents fluctuations on top of the mean-field solutions in the normal (superradiant) phase. Three regimes, denoted as I, II, and III, are identified based on the number of stable coexisting solutions. Subscripts 1 and 2 are employed to distinguish regimes with different Wigner distributions. The tricritical points are shown by blue triangles, and the multicritical points are marked by blue circles. The green curve in (b) indicates the unstable region (see details in Sec. S5 of [87]). (d) The Wigner functions in different regimes. Here, we consider the coordinates of λ and G/κ as I(1.0, 1.1), $\mathrm{II}_1(1.42, 2.6)$, $\mathrm{III}_1(1.8, 1.98)$, $\mathrm{II}_2(2.04, 2.24)$, and $\mathrm{III}_2(2.2, 2.42)$, $\Delta_q/\Delta = 1000$, and atomic decay $\gamma = \kappa$. (e) The critical lines at $\lambda = 2$ [the black dotted line in (a)] as a function of G. (f),(g) Cut plots of $\ln(\langle c^\dagger c\rangle + 1)$ [black dotted line in (b)] and $\ln(\langle d^\dagger d\rangle + 1)$ [black dotted line in (c)] as a function of λ. In (e)–(g), the blue solid and red dotted lines denote cavity fluctuations in the NP and SP, respectively. We consider $\Delta_F = 0$ in (a),(e), $\Delta_F/\Delta = 0.5$ in (b),(d),(f), and $\Delta_F/\Delta = -0.5$ in (c),(g).

left edge of the shaded region. Between these two critical pump strengths (within the shaded areas), if driven forward, the system is in the NP, while if driven backward, the system is in the SP. This phenomenon is called "nonreciprocal first-order superradiant phase transition".

In the right panels of Fig. 2, we fix $\lambda = 1.36$ and apply the forward and backward pumps, respectively. In this case, the cavity occupations exhibit continuous increase from zero to finite values at the critical pump strengths $G_{\mathrm{c,f}}^{\mathrm{second}} = 2.78\kappa$ and $G_{\mathrm{c,b}}^{\mathrm{second}} = 0.94\kappa$, respectively, as shown in Figs. 2(c) and 2(d). These results indicate a nonreciprocal *second-order* superradiant phase transition. Physically, the nonreciprocity originates from the opposite Sagnac shifts induced by the rotation of the cavity. This leads to a shift of the critical point for the forward (or backward) pump toward larger (or smaller) values [see Fig. S2(a) in [87]].

Nonreciprocal multicriticality.—To explore the steady-state fluctuations of the system, we adopt a semiclassical approach by displacing the cavity fields as $a \to \langle a\rangle + c$, $b \to \langle b\rangle + d$, where c and d are the annihilation operators that describe cavity fluctuations. In the large atomic detuning limit, we can obtain the effective low-energy Hamiltonian (see Sec. S2 in [87]),

$$H_{\mathrm{eff}} = \Lambda_1 c^\dagger c + \Lambda_2 d^\dagger d + [Gc^2 + \Lambda_3 c d^\dagger + \Lambda_4 e^{2i\phi} c^2 + \Lambda_5 e^{2i\phi} d^2 + \Lambda_6 e^{2i\phi} cd + \mathrm{H.c.}], \quad (5)$$

where the parameters Λ_n ($n = 1, 2, \ldots, 6$), ϕ are determined by the Sagnac shift Δ_F and the mean-field solutions α and β. In particular, the trivial solutions of $\alpha = \beta = 0$ correspond to the low-energy Hamiltonian in the normal phase. To analyze the nature of the nonreciprocal transitions in the open system, we combine Eq. (5) with the master equation (2) and obtain the steady-state solution of quantum fluctuations (see Sec. S4 in [87]).

Figures 3(a)–3(c) present the steady-state phase diagrams of photon number fluctuations. For a static cavity (i.e., $\Delta_F = 0$) [Fig. 3(a)], we observe two types of multicritical behaviors. There is a "tricritical point" denoted by the blue triangle where the first- and second-order critical lines meet, which is of the same type as in Refs. [34–36]. The other is the "multicritical point" denoted by the blue circle, where regimes I, II, and III coexist. Specially, these two critical lines, exhibiting different asymptotic behaviors [123], can morph into a divergent curve [see Fig. 3(e)]. Remarkably, this multicritical point shows nonreciprocal characteristics: in the forward pump, the multicritical point splits into two [see Fig. 3(b)], while in the backward pump and with the same atom-field coupling, the multicritical point disappears [see Fig. 3(c)]. Moreover, the cut plots of the phase diagram also show the nonreciprocity of the photon number fluctuations [see Figs. 3(f) and 3(g)].

To distinguish between regimes I, II, and III, in Fig. 3(d), we numerically calculate the Wigner functions of the cavity field using Hamiltonian in Eq. (1) [124,125], considering the detuning $\Delta_q/\Delta = 10^3$ and the nonzero atomic decay $\gamma = \kappa$. In the NP (regime I), the cavity field is almost in a vacuum state. In regime II_1, the Wigner function shows two peaks, reflecting the Z_2 symmetry breaking of the system. In regimes III_1 and III_2, the cavity fields are both squeezed, but with an orthogonal squeezing direction.

Possible implementations.—The proposed protocols could be implemented using either cold cesium atoms falling onto the surface of a WGM microdisk [77,78] or a single trapped ^{85}Rb atom interacts with a WGM microresonator [83] (see more details in Sec. S9. A of [87]). We consider the feasible parameters of the microresonator to be $Q = 6.0 \times 10^9$, $R = 1.1$ mm, $n = 1.4$, $\lambda_0 = 1550$ nm, and $\Omega = 6.6$ kHz [84], which yields a Sagnac shift of $\Delta_F = 3.2$ MHz and the intrinsic loss rate of $\kappa_i = 32$ kHz. The large atomic detuning required for the transition can be achieved by tuning the pump frequency $\omega_p \approx 2\omega_0$. We consider $\eta_+ = 100$, resulting in $\Delta = 6.4$ and $\Delta_q = 960$ MHz. Previous studies have shown that a detuning value of $\omega_q/\omega_0 = 50$ is sufficient to observe the superradiant transitions in NMR simulator [28] and trapped ion systems [29,30]. Based on the above parameters, the nonreciprocal first- and second-order superradiant transitions are predicted to occur at the atom-field couplings $g_a \approx 68$ and $g_b \approx 39$ MHz, which are experimentally feasible by adjusting the distance between the atom and the surface [83]. Additionally, the squeezed cavity mode can be generated using a periodically poled thin film of lithium niobate media [114,115]. Here, we consider the pump strength $G/\kappa = 2$, the external decay $\kappa_{\rm ex}^p = 2\kappa = 640$ kHz, and the coupling rate of the parametric nonlinear process ($g/\kappa = 0.001$ [115]), which yields the feasible critical pump power $P_c \approx 2.1$ nW.

Conclusions.—In summary, we have proposed a method for all-optical manipulating superradiant phase transitions and multicritical phenomena in an open dual-coupling JC model. The nonreciprocal first- and second-order superradiant transitions can be easily achieved by tuning the external pump field. Furthermore, the model allows for exquisite manipulation of the tricritical and multicritical points, both exhibiting controllable nonreciprocity. This general approach can be extended to the case of N particles ($N \gg 1$), specifically in the context of the dual-coupling Tavis-Cummings model (see Sec. S10 in [87]). We anticipate that this Letter will stimulate further theoretical studies and experimental explorations of a broader range of physical phenomena, such as superradiant cooling [126] and atomic synchronization [50,51], and could find applications in modern quantum technology [127].

We acknowledge valuable discussions with Ye-Xiong Zeng, Ran Huang, and Zi-Yong Ge. We also appreciate the valuable comments from Ye-Hong Chen, Zongping Gong, Keyu Xia, Bo Wang, and Zeliang Xiang. X.-Y. L. is supported by the National Key Research and Development Program of China (Grant No. 2021YFA1400700). F. N. is supported in part by Nippon Telegraph and Telephone Corporation (NTT) Research, the Japan Science and Technology Agency (JST) [via the Quantum Leap Flagship Program (Q-LEAP), and the Moonshot R&D Grant No. JPMJMS2061], the Asian Office of Aerospace Research and Development (AOARD) (via Grant No. FA2386-20-1-4069), and the Office of Naval Research (ONR) (via Grant No. N62909-23-1-2074). The computation is completed in the HPC Platform of Huazhong University of Science and Technology.

*xinyoulu@hust.edu.cn
†fnori@riken.jp

[1] C. Domb, *Phase Transitions and Critical Phenomena* (Elsevier, New York, 2000).
[2] S. Sachdev, *Quantum Phase Transitions* (Cambridge University Press, Cambridge, England, 2011).
[3] R. H. Dicke, Coherence in spontaneous radiation processes, Phys. Rev. **93**, 99 (1954).
[4] K. Hepp and E. H. Lieb, On the superradiant phase transition for molecules in a quantized radiation field: The Dicke maser model, Ann. Phys. (N.Y.) **76**, 360 (1973).
[5] Y. K. Wang and F. T. Hioe, Phase transition in the Dicke model of superradiance, Phys. Rev. A **7**, 831 (1973).
[6] C. Emary and T. Brandes, Quantum chaos triggered by precursors of a quantum phase transition: The Dicke model, Phys. Rev. Lett. **90**, 044101 (2003).
[7] N. Lambert, C. Emary, and T. Brandes, Entanglement and the phase transition in single-mode superradiance, Phys. Rev. Lett. **92**, 073602 (2004).
[8] F. Dimer, B. Estienne, A. S. Parkins, and H. J. Carmichael, Proposed realization of the Dicke-model quantum phase transition in an optical cavity QED system, Phys. Rev. A **75**, 013804 (2007).
[9] K. Baumann, C. Guerlin, F. Brennecke, and T. Esslinger, Dicke quantum phase transition with a superfluid gas in an optical cavity, Nature (London) **464**, 1301 (2010).
[10] M. P. Baden, K. J. Arnold, A. L. Grimsmo, S. Parkins, and M. D. Barrett, Realization of the Dicke model using cavity-assisted Raman transitions, Phys. Rev. Lett. **113**, 020408 (2014).
[11] D. Nagy, G. Kónya, G. Szirmai, and P. Domokos, Dicke-model phase transition in the quantum motion of a Bose-Einstein condensate in an optical cavity, Phys. Rev. Lett. **104**, 130401 (2010).
[12] X.-Y. Lü, L.-L. Zheng, G.-L. Zhu, and Y. Wu, Single-photon-triggered quantum phase transition, Phys. Rev. Appl. **9**, 064006 (2018).
[13] P. Kirton, M. M. Roses, J. Keeling, and E. G. Dalla Torre, Introduction to the Dicke model: From equilibrium to nonequilibrium, and vice versa, Adv. Quantum Technol. **2**, 1800043 (2019).
[14] Y. Xu, D. Fallas Padilla, and H. Pu, Multicriticality and quantum fluctuation in a generalized Dicke model, Phys. Rev. A **104**, 043708 (2021).
[15] J. Zhao and M.-J. Hwang, Frustrated superradiant phase transition, Phys. Rev. Lett. **128**, 163601 (2022).
[16] I. I. Rabi, Space quantization in a gyrating magnetic field, Phys. Rev. **51**, 652 (1937).
[17] D. Braak, Integrability of the Rabi model, Phys. Rev. Lett. **107**, 100401 (2011).

[18] Q. Xie, H. Zhong, M. T. Batchelor, and C. Lee, The quantum Rabi model: Solution and dynamics, J. Phys. A **50**, 113001 (2017).
[19] M.-J. Hwang, R. Puebla, and M. B. Plenio, Quantum phase transition and universal dynamics in the Rabi model, Phys. Rev. Lett. **115**, 180404 (2015).
[20] M. Liu, S. Chesi, Z.-J. Ying, X. Chen, H.-G. Luo, and H.-Q. Lin, Universal scaling and critical exponents of the anisotropic quantum Rabi model, Phys. Rev. Lett. **119**, 220601 (2017).
[21] X.-Y. Lü, G.-L. Zhu, L.-L. Zheng, and Y. Wu, Entanglement and quantum superposition induced by a single photon, Phys. Rev. A **97**, 033807 (2018).
[22] M.-J. Hwang, P. Rabl, and M. B. Plenio, Dissipative phase transition in the open quantum Rabi model, Phys. Rev. A **97**, 013825 (2018).
[23] Y.-Y. Zhang, Z.-X. Hu, L. Fu, H.-G. Luo, H. Pu, and X.-F. Zhang, Quantum phases in a quantum Rabi triangle, Phys. Rev. Lett. **127**, 063602 (2021).
[24] D. Fallas Padilla, H. Pu, G.-J. Cheng, and Y.-Y. Zhang, Understanding the quantum Rabi ring using analogies to quantum magnetism, Phys. Rev. Lett. **129**, 183602 (2022).
[25] J. Liu, M. Zhao, Y.-T. Yang, and H.-G. Luo, Using nonclassical states to explore the superradiant phase transition in the quantum Rabi model, Phys. Rev. A **109**, 023721 (2024).
[26] L.-T. Shen, C.-Q. Tang, Z. Shi, H. Wu, Z.-B. Yang, and S.-B. Zheng, Squeezed-light-induced quantum phase transition in the Jaynes-Cummings model, Phys. Rev. A **106**, 023705 (2022).
[27] I. M. Georgescu, S. Ashhab, and F. Nori, Quantum simulation, Rev. Mod. Phys. **86**, 153 (2014).
[28] X. Chen, Z. Wu, M. Jiang, X.-Y. Lü, X. Peng, and J. Du, Experimental quantum simulation of superradiant phase transition beyond no-go theorem via antisqueezing, Nat. Commun. **12**, 6281 (2021).
[29] R. Puebla, M.-J. Hwang, J. Casanova, and M. B. Plenio, Probing the dynamics of a superradiant quantum phase transition with a single trapped ion, Phys. Rev. Lett. **118**, 073001 (2017).
[30] M.-L. Cai, Z.-D. Liu, W.-D. Zhao, Y.-K. Wu, Q.-X. Mei, Y. Jiang, L. He, X. Zhang, Z.-C. Zhou, and L.-M. Duan, Observation of a quantum phase transition in the quantum Rabi model with a single trapped ion, Nat. Commun. **12**, 1126 (2021).
[31] R.-H. Zheng, W. Ning, Y.-H. Chen, J.-H. Lü, L.-T. Shen, K. Xu, Y.-R. Zhang, D. Xu, H. Li, Y. Xia, F. Wu, Z.-B. Yang, A. Miranowicz, N. Lambert, D. Zheng, H. Fan, F. Nori, and S.-B. Zheng, Observation of a superradiant phase transition with emergent cat states, Phys. Rev. Lett. **131**, 113601 (2023).
[32] P. Kirton and J. Keeling, Suppressing and restoring the Dicke superradiance transition by dephasing and decay, Phys. Rev. Lett. **118**, 123602 (2017).
[33] N. Shammah, S. Ahmed, N. Lambert, S. De Liberato, and F. Nori, Open quantum systems with local and collective incoherent processes: Efficient numerical simulations using permutational invariance, Phys. Rev. A **98**, 063815 (2018).
[34] M. Soriente, T. Donner, R. Chitra, and O. Zilberberg, Dissipation-induced anomalous multicritical phenomena, Phys. Rev. Lett. **120**, 183603 (2018).
[35] C. J. Zhu, L. L. Ping, Y. P. Yang, and G. S. Agarwal, Squeezed light induced symmetry breaking superradiant phase transition, Phys. Rev. Lett. **124**, 073602 (2020).
[36] R. Lin, R. Rosa-Medina, F. Ferri, F. Finger, K. Kroeger, T. Donner, T. Esslinger, and R. Chitra, Dissipation-engineered family of nearly dark states in many-body cavity-atom systems, Phys. Rev. Lett. **128**, 153601 (2022).
[37] Y. Xu and H. Pu, Emergent universality in a quantum tricritical Dicke model, Phys. Rev. Lett. **122**, 193201 (2019).
[38] H.-J. Zhu, K. Xu, G.-F. Zhang, and W.-M. Liu, Finite-component multicriticality at the superradiant quantum phase transition, Phys. Rev. Lett. **125**, 050402 (2020).
[39] J. Larson and E. K. Irish, Some remarks on "superradiant" phase transitions in light-matter systems, J. Phys. A **50**, 174002 (2017).
[40] H. J. Carmichael, Breakdown of photon blockade: A dissipative quantum phase transition in zero dimensions, Phys. Rev. X **5**, 031028 (2015).
[41] J. M. Fink, A. Dombi, A. Vukics, A. Wallraff, and P. Domokos, Observation of the photon-blockade breakdown phase transition, Phys. Rev. X **7**, 011012 (2017).
[42] F. Reiter, T. L. Nguyen, J. P. Home, and S. F. Yelin, Cooperative breakdown of the oscillator blockade in the Dicke model, Phys. Rev. Lett. **125**, 233602 (2020).
[43] D. Meiser, J. Ye, D. R. Carlson, and M. J. Holland, Prospects for a millihertz-linewidth laser, Phys. Rev. Lett. **102**, 163601 (2009).
[44] J. G. Bohnet, Z. Chen, J. M. Weiner, D. Meiser, M. J. Holland, and J. K. Thompson, A steady-state superradiant laser with less than one intracavity photon, Nature (London) **484**, 78 (2012).
[45] M. A. Norcia and J. K. Thompson, Cold-strontium laser in the superradiant crossover regime, Phys. Rev. X **6**, 011025 (2016).
[46] M. A. Norcia, M. N. Winchester, J. R. Cline, and J. K. Thompson, Superradiance on the millihertz linewidth strontium clock transition, Sci. Adv. **2**, e1601231 (2016).
[47] Z. Gong, R. Hamazaki, and M. Ueda, Discrete time-crystalline order in cavity and circuit QED systems, Phys. Rev. Lett. **120**, 040404 (2018).
[48] R. Mattes, I. Lesanovsky, and F. Carollo, Entangled time-crystal phase in an open quantum light-matter system, Phys. Rev. A **108**, 062216 (2023).
[49] G. Ferioli, A. Glicenstein, I. Ferrier-Barbut, and A. Browaeys, A non-equilibrium superradiant phase transition in free space, Nat. Phys. **19**, 1345 (2023).
[50] M. Xu, D. A. Tieri, E. C. Fine, J. K. Thompson, and M. J. Holland, Synchronization of two ensembles of atoms, Phys. Rev. Lett. **113**, 154101 (2014).
[51] S. J. Masson and A. Asenjo-Garcia, Universality of Dicke superradiance in arrays of quantum emitters, Nat. Commun. **13**, 2285 (2022).
[52] Z. Lin, H. Ramezani, T. Eichelkraut, T. Kottos, H. Cao, and D. N. Christodoulides, Unidirectional invisibility induced by $\mathcal{PT}$-symmetric periodic structures, Phys. Rev. Lett. **106**, 213901 (2011).

[53] B. Peng, Ş. K. Özdemir, F. Lei, F. Monifi, M. Gianfreda, G. L. Long, S. Fan, F. Nori, C. M. Bender, and L. Yang, Parity–time-symmetric whispering-gallery microcavities, Nat. Phys. **10**, 394 (2014).

[54] L. Chang, X. Jiang, S. Hua, C. Yang, J. Wen, L. Jiang, G. Li, G. Wang, and M. Xiao, Parity–time symmetry and variable optical isolation in active–passive-coupled microresonators, Nat. Photonics **8**, 524 (2014).

[55] L. Fan, J. Wang, L. T. Varghese, H. Shen, B. Niu, Y. Xuan, A. M. Weiner, and M. Qi, An all-silicon passive optical diode, Science **335**, 447 (2012).

[56] Q.-T. Cao, H. Wang, C.-H. Dong, H. Jing, R.-S. Liu, X. Chen, L. Ge, Q. Gong, and Y.-F. Xiao, Experimental demonstration of spontaneous chirality in a nonlinear microresonator, Phys. Rev. Lett. **118**, 033901 (2017).

[57] S. Manipatruni, J. T. Robinson, and M. Lipson, Optical nonreciprocity in optomechanical structures, Phys. Rev. Lett. **102**, 213903 (2009).

[58] Z. Shen, Y.-L. Zhang, Y. Chen, C.-L. Zou, Y.-F. Xiao, X.-B. Zou, F.-W. Sun, G.-C. Guo, and C.-H. Dong, Experimental realization of optomechanically induced non-reciprocity, Nat. Photonics **10**, 657 (2016).

[59] D.-W. Wang, H.-T. Zhou, M.-J. Guo, J.-X. Zhang, J. Evers, and S.-Y. Zhu, Optical diode made from a moving photonic crystal, Phys. Rev. Lett. **110**, 093901 (2013).

[60] H. Ramezani, P. K. Jha, Y. Wang, and X. Zhang, Nonreciprocal localization of photons, Phys. Rev. Lett. **120**, 043901 (2018).

[61] S. Zhang, Y. Hu, G. Lin, Y. Niu, K. Xia, J. Gong, and S. Gong, Thermal-motion-induced non-reciprocal quantum optical system, Nat. Photonics **12**, 744 (2018).

[62] K. Xia, F. Nori, and M. Xiao, Cavity-free optical isolators and circulators using a chiral cross-Kerr nonlinearity, Phys. Rev. Lett. **121**, 203602 (2018).

[63] L. Tang, J. Tang, M. Chen, F. Nori, M. Xiao, and K. Xia, Quantum squeezing induced optical nonreciprocity, Phys. Rev. Lett. **128**, 083604 (2022).

[64] C. H. Bennett and D. P. DiVincenzo, Quantum information and computation, Nature (London) **404**, 247 (2000).

[65] I. Buluta, S. Ashhab, and F. Nori, Natural and artificial atoms for quantum computation, Rep. Prog. Phys. **74**, 104401 (2011).

[66] H. J. Kimble, The quantum internet, Nature (London) **453**, 1023 (2008).

[67] M. Fruchart, R. Hanai, P. B. Littlewood, and V. Vitelli, Non-reciprocal phase transitions, Nature (London) **592**, 363 (2021).

[68] Ezequiel I. Rodríguez Chiacchio, A. Nunnenkamp, and M. Brunelli, Nonreciprocal Dicke model, Phys. Rev. Lett. **131**, 113602 (2023).

[69] F. Ferri, R. Rosa-Medina, F. Finger, N. Dogra, M. Soriente, O. Zilberberg, T. Donner, and T. Esslinger, Emerging dissipative phases in a superradiant quantum gas with tunable decay, Phys. Rev. X **11**, 041046 (2021).

[70] J. Klinder, H. Keßler, M. Wolke, L. Mathey, and A. Hemmerich, Dynamical phase transition in the open Dicke model, Proc. Natl. Acad. Sci. U.S.A. **112**, 3290 (2015).

[71] Z. Zhiqiang, C. H. Lee, R. Kumar, K. Arnold, S. J. Masson, A. Parkins, and M. Barrett, Nonequilibrium phase transition in a spin-1 Dicke model, Optica **4**, 424 (2017).

[72] M. Feng, Y. Zhong, T. Liu, L. Yan, W. Yang, J. Twamley, and H. Wang, Exploring the quantum critical behaviour in a driven Tavis–Cummings circuit, Nat. Commun. **6**, 7111 (2015).

[73] L. Garbe, M. Bina, A. Keller, M. G. A. Paris, and S. Felicetti, Critical quantum metrology with a finite-component quantum phase transition, Phys. Rev. Lett. **124**, 120504 (2020).

[74] Y. Chu, S. Zhang, B. Yu, and J. Cai, Dynamic framework for criticality-enhanced quantum sensing, Phys. Rev. Lett. **126**, 010502 (2021).

[75] Z.-J. Ying, S. Felicetti, G. Liu, and D. Braak, Critical quantum metrology in the non-linear quantum Rabi model, Entropy **24**, 1015 (2022).

[76] W.-T. He, C.-W. Lu, Y.-X. Yao, H.-Y. Zhu, and Q. Ai, Criticality-based quantum metrology in the presence of decoherence, Front. Phys. **18**, 31304 (2023).

[77] T. Aoki, B. Dayan, E. Wilcut, W. P. Bowen, A. S. Parkins, T. Kippenberg, K. Vahala, and H. Kimble, Observation of strong coupling between one atom and a monolithic microresonator, Nature (London) **443**, 671 (2006).

[78] D. Alton, N. Stern, T. Aoki, H. Lee, E. Ostby, K. Vahala, and H. Kimble, Strong interactions of single atoms and photons near a dielectric boundary, Nat. Phys. **7**, 159 (2011).

[79] C. Junge, D. O'Shea, J. Volz, and A. Rauschenbeutel, Strong coupling between single atoms and nontransversal photons, Phys. Rev. Lett. **110**, 213604 (2013).

[80] I. Shomroni, S. Rosenblum, Y. Lovsky, O. Bechler, G. Guendelman, and B. Dayan, All-optical routing of single photons by a one-atom switch controlled by a single photon, Science **345**, 903 (2014).

[81] M. Scheucher, A. Hilico, E. Will, J. Volz, and A. Rauschenbeutel, Quantum optical circulator controlled by a single chirally coupled atom, Science **354**, 1577 (2016).

[82] O. Bechler, A. Borne, S. Rosenblum, G. Guendelman, O. E. Mor, M. Netser, T. Ohana, Z. Aqua, N. Drucker, R. Finkelstein, Y. Lovsky, R. Bruch, D. Gurovich, E. Shafir, and B. Dayan, A passive photon–atom qubit swap operation, Nat. Phys. **14**, 996 (2018).

[83] E. Will, L. Masters, A. Rauschenbeutel, M. Scheucher, and J. Volz, Coupling a single trapped atom to a whispering-gallery-mode microresonator, Phys. Rev. Lett. **126**, 233602 (2021).

[84] S. Maayani, R. Dahan, Y. Kligerman, E. Moses, A. U. Hassan, H. Jing, F. Nori, D. N. Christodoulides, and T. Carmon, Flying couplers above spinning resonators generate irreversible refraction, Nature (London) **558**, 569 (2018).

[85] K. Y. Bliokh and F. Nori, Transverse and longitudinal angular momenta of light, Phys. Rep. **592**, 1 (2015).

[86] K. Y. Bliokh, D. Smirnova, and F. Nori, Quantum spin Hall effect of light, Science **348**, 1448 (2015).

[87] See Supplemental Material at http://link.aps.org/supplemental/10.1103/PhysRevLett.132.193602, for additional details on the discussions of phase transitions, numerical simulations, and potential experimental implementations, which includes Refs. [88–109].

[88] S. Ashhab and F. Nori, Qubit-oscillator systems in the ultrastrong-coupling regime and their potential for preparing nonclassical states, Phys. Rev. A **81**, 042311 (2010).
[89] S. Ashhab, Superradiance transition in a system with a single qubit and a single oscillator, Phys. Rev. A **87**, 013826 (2013).
[90] R. Puebla, M.-J. Hwang, and M. B. Plenio, Excited-state quantum phase transition in the Rabi model, Phys. Rev. A **94**, 023835 (2016).
[91] Z. Wang, Y. Chong, J. D. Joannopoulos, and M. Soljačić, Observation of unidirectional backscattering-immune topological electromagnetic states, Nature (London) **461**, 772 (2009).
[92] A. B. Khanikaev, S. H. Mousavi, G. Shvets, and Y. S. Kivshar, One-way extraordinary optical transmission and nonreciprocal spoof plasmons, Phys. Rev. Lett. **105**, 126804 (2010).
[93] D. Dai, J. Bauters, and J. E. Bowers, Passive technologies for future large-scale photonic integrated circuits on silicon: Polarization handling, light non-reciprocity and loss reduction, Light Sci. Appl. **1**, e1 (2012).
[94] G. Kurizki, P. Bertet, Y. Kubo, K. Mølmer, D. Petrosyan, P. Rabl, and J. Schmiedmayer, Quantum technologies with hybrid systems, Proc. Natl. Acad. Sci. U.S.A. **112**, 3866 (2015).
[95] J. Ward and O. Benson, WGM microresonators: Sensing, lasing and fundamental optics with microspheres, Laser Photonics Rev. **5**, 553 (2011).
[96] M. Jinno and T. Matsumoto, Ultrafast, low power, and highly stable all-optical switching in an all polarization maintaining fiber Sagnac interferometer, IEEE Photonics Technol. Lett. **2**, 349 (1990).
[97] B. Dayan, A. Parkins, T. Aoki, E. Ostby, K. Vahala, and H. Kimble, A photon turnstile dynamically regulated by one atom, Science **319**, 1062 (2008).
[98] T. Aoki, A. S. Parkins, D. J. Alton, C. A. Regal, B. Dayan, E. Ostby, K. J. Vahala, and H. J. Kimble, Efficient routing of single photons by one atom and a microtoroidal cavity, Phys. Rev. Lett. **102**, 083601 (2009).
[99] A. Kiraz, P. Michler, C. Becher, B. Gayral, A. Imamoğlu, L. Zhang, E. Hu, W. Schoenfeld, and P. Petroff, Cavity-quantum electrodynamics using a single In As quantum dot in a microdisk structure, Appl. Phys. Lett. **78**, 3932 (2001).
[100] E. Peter, P. Senellart, D. Martrou, A. Lemaître, J. Hours, J. M. Gérard, and J. Bloch, Exciton-photon strong-coupling regime for a single quantum dot embedded in a microcavity, Phys. Rev. Lett. **95**, 067401 (2005).
[101] K. Srinivasan and O. Painter, Linear and nonlinear optical spectroscopy of a strongly coupled microdisk–quantum dot system, Nature (London) **450**, 862 (2007).
[102] K. Srinivasan and O. Painter, Mode coupling and cavity–quantum-dot interactions in a fiber-coupled microdisk cavity, Phys. Rev. A **75**, 023814 (2007).
[103] Y.-S. Park, A. K. Cook, and H. Wang, Cavity QED with diamond nanocrystals and silica microspheres, Nano Lett. **6**, 2075 (2006).
[104] R. J. Barbour, K. N. Dinyari, and H. Wang, A composite microcavity of diamond nanopillar and deformed silica microsphere with enhanced evanescent decay length, Opt. Express **18**, 18968 (2010).
[105] J. U. Fürst, D. V. Strekalov, D. Elser, A. Aiello, U. L. Andersen, C. Marquardt, and G. Leuchs, Quantum light from a whispering-gallery-mode disk resonator, Phys. Rev. Lett. **106**, 113901 (2011).
[106] V. S. Ilchenko, A. A. Savchenkov, A. B. Matsko, and L. Maleki, Nonlinear optics and crystalline whispering gallery mode cavities, Phys. Rev. Lett. **92**, 043903 (2004).
[107] T. Beckmann, H. Linnenbank, H. Steigerwald, B. Sturman, D. Haertle, K. Buse, and I. Breunig, Highly tunable low-threshold optical parametric oscillation in radially poled whispering gallery resonators, Phys. Rev. Lett. **106**, 143903 (2011).
[108] M. Förtsch, J. U. Fürst, C. Wittmann, D. Strekalov, A. Aiello, M. V. Chekhova, C. Silberhorn, G. Leuchs, and C. Marquardt, A versatile source of single photons for quantum information processing, Nat. Commun. **4**, 1818 (2013).
[109] X. Guo, C.-L. Zou, H. Jung, and H. X. Tang, On-chip strong coupling and efficient frequency conversion between telecom and visible optical modes, Phys. Rev. Lett. **117**, 123902 (2016).
[110] H. Jing, H. Lü, S. K. Özdemir, T. Carmon, and F. Nori, Nanoparticle sensing with a spinning resonator, Optica **5**, 1424 (2018).
[111] R. Huang, A. Miranowicz, J.-Q. Liao, F. Nori, and H. Jing, Nonreciprocal photon blockade, Phys. Rev. Lett. **121**, 153601 (2018).
[112] Y.-F. Jiao, S.-D. Zhang, Y.-L. Zhang, A. Miranowicz, L.-M. Kuang, and H. Jing, Nonreciprocal optomechanical entanglement against backscattering losses, Phys. Rev. Lett. **125**, 143605 (2020).
[113] C. Hotter, H. Ritsch, and K. Gietka, Combining critical and quantum metrology, Phys. Rev. Lett. **132**, 060801 (2024).
[114] J. Lu, J. B. Surya, X. Liu, A. W. Bruch, Z. Gong, Y. Xu, and H. X. Tang, Periodically poled thin-film lithium niobate microring resonators with a second-harmonic generation efficiency of 250,000%/w, Optica **6**, 1455 (2019).
[115] J. Lu, M. Li, C.-L. Zou, A. Al Sayem, and H. X. Tang, Toward 1% single-photon anharmonicity with periodically poled lithium niobate microring resonators, Optica **7**, 1654 (2020).
[116] M. O. Scully and M. S. Zubairy, *Quantum Optics* (Cambridge University Press, Cambridge, England, 1999).
[117] G. S. Agarwal, *Quantum Optics* (Cambridge University Press, Cambridge, England, 2012).
[118] S. Huang and G. S. Agarwal, Normal-mode splitting in a coupled system of a nanomechanical oscillator and a parametric amplifier cavity, Phys. Rev. A **80**, 033807 (2009).
[119] X.-Y. Lü, Y. Wu, J. R. Johansson, H. Jing, J. Zhang, and F. Nori, Squeezed optomechanics with phase-matched amplification and dissipation, Phys. Rev. Lett. **114**, 093602 (2015).
[120] W. Qin, A. Miranowicz, P.-B. Li, X.-Y. Lü, J. Q. You, and F. Nori, Exponentially enhanced light-matter interaction, cooperativities, and steady-state entanglement using parametric amplification, Phys. Rev. Lett. **120**, 093601 (2018).

[121] W. Qin, A. Miranowicz, and F. Nori, Beating the 3 db limit for intracavity squeezing and its application to nondemolition qubit readout, Phys. Rev. Lett. **129**, 123602 (2022).

[122] G. B. Malykin, The Sagnac effect: Correct and incorrect explanations, Phys. Usp. **43**, 1229 (2000).

[123] D. Nagy, G. Szirmai, and P. Domokos, Critical exponent of a quantum-noise-driven phase transition: The open-system Dicke model, Phys. Rev. A **84**, 043637 (2011).

[124] J. Johansson, P. Nation, and F. Nori, Qutip: An open-source PYTHON framework for the dynamics of open quantum systems, Comput. Phys. Commun. **183**, 1760 (2012).

[125] J. Johansson, P. Nation, and F. Nori, Qutip 2: A PYTHON framework for the dynamics of open quantum systems, Comput. Phys. Commun. **184**, 1234 (2013).

[126] M. Xu, S. B. Jäger, S. Schütz, J. Cooper, G. Morigi, and M. J. Holland, Supercooling of atoms in an optical resonator, Phys. Rev. Lett. **116**, 153002 (2016).

[127] S. L. Braunstein and P. van Loock, Quantum information with continuous variables, Rev. Mod. Phys. **77**, 513 (2005).